

**Properties of rice straw reinforced alkali activated
cementitious composites**

NGUYEN, C.V. and MANGAT, Pal <<http://orcid.org/0000-0003-1736-8891>>

Available from Sheffield Hallam University Research Archive (SHURA) at:

<http://shura.shu.ac.uk/27539/>

This document is the author deposited version. You are advised to consult the publisher's version if you wish to cite from it.

Published version

NGUYEN, C.V. and MANGAT, Pal (2020). Properties of rice straw reinforced alkali activated cementitious composites. *Construction and Building Materials*, 261, p. 120536.

Copyright and re-use policy

See <http://shura.shu.ac.uk/information.html>

1 Properties of rice straw reinforced alkali activated cementitious composites

2
3 Chinh Van Nguyen^{a,b}, P.S. Mangat^{a*}

4 ^a Centre for Infrastructure Management, Materials and Engineering Research Institute,
5 Sheffield Hallam University, Sheffield S1 1WB, UK

6 ^b Faculty of Civil Engineering, The University of Danang- University of Science and
7 Technology, 54 Nguyen Luong Bang, Danang, Vietnam

8 *Corresponding author: P.S. Mangat, Email address: p.s.mangat@shu.ac.uk; Tel:
9 +44(0)1142253339

10
11 Co-authors: Chinh Van Nguyen , E-mail address: chinhx1a@gmail.com;
12 nvchinh@dut.udn.vn; Tel: +84 (0) 9011 22 777; ORCID: 0000-0002-7953-5731
13

14 15 **HIGHLIGHTS**

- 16 • Characteristics of rice straw were studied by SEMs and XRDs
- 17 • Characteristics of rice straw alkali activated cementitious composites were investigated via
18 strengths, density, water absorption, drying shrinkage and wet/dry cycling.
- 19 • Alkali treatment enhances bond at rice straw and alkali activated cementitious paste interface
- 20 • Mechanisms of deterioration of the composites under wet/dry cycling was studied by SEMs

34 **Properties of rice straw reinforced alkali activated cementitious composites** 35 **ABSTRACT**

36 The paper investigates the characteristics of rice straw reinforced alkali activated cementitious
37 composites (AACC). The untreated and NaOH treated rice straw at the proportion of 1%, 2%,
38 3% by weight of binder was added to the mixes. Characteristics of rice straw have been
39 studied by using SEM and XRD. Mechanical properties, water absorption, drying shrinkage
40 and durability under wet/dry cycling have been investigated to evaluate the performance of
41 the AACCs. SEM was also used to investigate the mechanism of deterioration of the AACC.
42 The results show that rice straw has very significant positive effects on the performance of
43 AACCs including increase in flexural and compressive strength, durability under wet/dry
44 cycling, large reduction in drying shrinkage, and water absorption. In addition, alkali
45 treatment is an effective method for enhancing bond between the rice straw and the matrix
46 leading to improved performance of AACCs.

47 **Keywords:** Alkali activated cementitious composite (AACC); Rice straw; Alkali treatment;
48 Strength; Durability; Drying shrinkage; Water absorption.

49 **1. Introduction**

50 CO₂ emission is a key contribute to global warming and the production of Portland cement
51 provides about 5% of global CO₂ emission [1]. Efforts to reduce the use of Portland cement in
52 concrete have led to research on alkali activated cementitious materials (AACMs) in order to
53 provide sustainable material for the construction industry. Alkali activation is the chemical
54 reaction between a solid aluminosilicate precursor and an alkaline activator to make hardened
55 materials. The curing temperature mainly depends on the content of calcium within the
56 aluminosilicate. The alkali activated aluminosilicate containing high calcium content can be
57 hardened at ambient temperature; whereas thermal treatment should be applied to induce the
58 setting of alkali activated aluminosilicate without calcium source [2-4]. The main precursors
59 used for producing AACMs are industrial by products such as granulated blast furnace slag
60 derived from the steel manufacture, fly ash derived from coal combustion and natural clays
61 (metakaolin) [5].

62 Characteristics of alkali activated cementitious materials have been studied by many
63 researchers. Compressive strengths of alkali-activated, blast furnace slag high-calcium binders
64 and fly ash-based low-calcium binders can be achieved up to 110MPa [6]. Drying shrinkage
65 of AACMs is typically higher than that of Portland cement-based binders, when
66 manufactured and cured under ambient temperatures, but can be controlled by good mix
67 design of the AACM concrete [3,7] or by using shrinkage reducing admixtures [8]. The
68 sorptivity of AACMs is within a comparable range with similar grade concretes [4]. The
69 capillary sorptivity is reduced by employing a lower water content and a higher silica
70 modulus activator [3]. AACM shows greater durability potential than OPC as it has lower
71 porosity [9]. Some tests have shown that superior chloride resistance of the AACM concrete
72 compared with a similar grade of normal Portland cement-based concrete [7]. Carbonation
73 results of AACMs under accelerated carbonation testing often show inferior performance to
74 Portland cement binders, which contradict data obtained under long-term natural exposure [4].
75 Many studies have shown better frost resistance of AACM concrete compared with similar
76 grade conventional concretes exposed to the same conditions [10,11].

77 Natural fibres have been used to replace synthetic fibres to reinforce concrete or mortar for
78 sustainable development. The natural fibres including sisal, flax, hemp, bamboo and coir are

79 cheaper and lighter than synthetic fibres. They are an abundant, renewable and low cost
80 resource [12-15]. There has been far less research on cellulose fibre reinforced cement
81 composites compared with synthetic fibres. The main drawbacks for the use of cellulose
82 fibres as reinforcement for cement composites are the shortage of information on production
83 techniques, failure mechanism, fibre strength, effectiveness of fibre shape and size on the
84 performance of composites [16]. Therefore, it is necessary to conduct more research on the
85 performance of cellulose fibre reinforced cement composites, including the effect of fibre
86 dispersion on the matrix properties.

87 Rice straw is a worldwide by-product of rice production. There are some current solutions for
88 disposal of rice straw such as livestock feeds, burning in-situ in the farm or incorporating into
89 the soil. Each solution shows its own advantages and disadvantages. Burning at the field is
90 considered as the cheapest method but it causes air pollution as it releases CO₂ [17]. The use
91 of rice straw to provide natural fibres has been studied and rice straw shows a high potential
92 for fibre reinforcement in cementitious mortar and concrete [17-19].

93 The paper investigates the characteristics of a novel alkali activated cementitious composite
94 (AACC) for low impact buildings by incorporating rice straw fibres from agricultural waste
95 products. The characteristics of rice straw have been determined by Scanning Electron
96 Microscope (SEM) and X-ray powder diffraction (XRD). The performance of AACC has
97 been investigated with a wide range of tests including compressive strength, flexural strength,
98 water absorption, drying shrinkage and durability under wet/dry cycling. A SEM was used to
99 study the bond at the rice straw interface with the alkali activated cementitious matrix in order
100 to explain its influence on strength and durability of the composites material. In addition,
101 XRD analysis was also used to determine the effect of chemical reaction between rice straw
102 and AACM matrix on the crystalline structure of the matrix.

103 2. Experimental programme

104 2.1 Materials

105 The alkali activated cementitious composites consists of ground granulated blast furnace slag
106 (GGBS) based binder, fine aggregate (sand), sodium silicate and hydroxide based activator,
107 retarder R42 and rice straw (RS) fibres. The activator was based on a sodium silicate solution
108 of molarity 6.5 mol/L and silica modulus 2% together with NaOH of molarity 4.8 mol/L.
109 GGBS was supplied by Hanson Heidelberg cement Group, UK and its chemical composition
110 is shown in **Table 1**. The XRD pattern of GGBS is presented in **Fig. 1** which was obtained by
111 using a Philips X-1 Pert X-ray diffractometer, operated with a Cu K α radiation source (40 KV
112 and 40 mA, wavelength $\lambda=1.5406\text{nm}$ [6.07×10^{-9} 2 in.]) by scanning from 5° to 75° at an
113 angle of 2 θ , the scan step size is 0.0131303. X-ray data were fitted using the pseudo-Voigt
114 profile function and refined by means of Rietveld. The GGBS shows a peak hump between
115 2 θ =20° and 40° because of the amorphous components. **Fig.1** also shows that there is no
116 significant crystalline material observed. Fine aggregate (sand) obtained from a supplier in
117 Sheffield, UK was oven dried at 60°C for 24hours. It was sieved to remove particles retained
118 on a 2mm size sieve then left in the laboratory air for three days before mixing and casting.
119

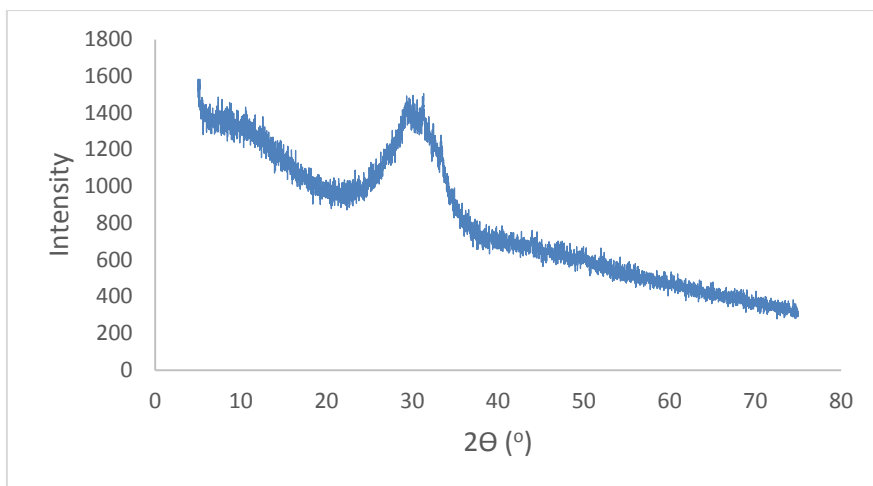


Fig. 1. X-Ray diffractograms of GGBS

120
121
122
123
124
125
126
127
128
129
130
131
132
133

Rice straw was received from a supplier in China. It was cut into 15-20mm lengths by using a scissors and classified as two types of fibre namely untreated rice straw (URS) and treated rice straw (TRS). For untreated fibre, the chopped rice straw was stored in an air tight bag until its use. For treated fibre, the chopped rice straw was soaked in 5%NaOH solution for 48hours in a fume cupboard, then washed with tap water until clear and oven dried at 45°C for 24 hours. The fibre was left in the laboratory air for 24hours and then sealed in an air tight bag until its use in the AACC mixes (see **Fig. 2**). This alkali treatment has proved to be effective for eliminating organic impurities and low molar mass hemicellulose thereby enhancing the fibre strength and fibre-matrix adhesion [13, 20, 21] including rice straw [18]. This treatment method also breaks down fibre bundles into thinner fibres, thereby, increasing their effective surface area [22] as can be seen in **Fig. 2**. **No additional physical treatment was applied to thin up the straw fibres.**



134
135
136
137
138
139
140
141
142
143

Fig. 2. (a) Untreated and (b) treated rice straw fibres

144 **Table 1**
 145 Chemical composition of GGBS

Constituents	GGBS
Na ₂ O %	0.786
MgO %	11.122
Al ₂ O ₃ %	16.352
SiO ₂ %	32.972
SO ₃ %	2.109
K ₂ O %	0.667
CaO %	34.919
TiO ₂ %	0.24
MnO %	0.265
Fe ₂ O ₃ %	0.17
SrO %	0.154
BaO %	0.244

146 **2.2 Details of mixes**

147 Details of all mixes are given in **Table 2**. The mix composition of the control sample (M0) are
 148 1: 1.94 (by weight) of binder to sand with liquid activator/binder of 0.56 and extra
 149 water/binder of 0.1. Extra water was used to improve the workability of the rice straw
 150 composites and also to compensate for the dry state of fine aggregate and fibre. The retarder
 151 R42 at ratio of 0.76% by weight of binder was added to the mix for increasing the setting
 152 time. The URS and TRS fibres were added at 1%, 2% and 3% of total binder weight, to
 153 produce composite mixes M1U, M2U, M3U and M1T, M2T, M3T respectively. The rice
 154 straw was used to replace its weight of sand in all mixes.

155 **Table 2**
 156 The mix proportions of AACM

ID	AACM Binder (%)	Sand (%)	R42 (% binder)	Liquid activator/ Binder Ratio	Water/ Binder Ratio	Rice straw	
						Amount (%Binder)	Treatment methods
M0	34	66.00	0.76	0.56	0.1	0	-
M1U	34	65.94	0.76	0.56	0.1	1	untreated
M2U	34	65.89	0.76	0.56	0.1	2	untreated
M3U	34	65.83	0.76	0.56	0.1	3	untreated
M1T	34	65.94	0.76	0.56	0.1	1	treated NaOH
M2T	34	65.89	0.76	0.56	0.1	2	treated NaOH
M3T	34	65.83	0.76	0.56	0.1	3	treated NaOH

157 **2.3. Casting and curing**

158 The AACM binder and sand were mixed for one minute and then the liquid activator was
 159 slowly added to the mix. Mixing continued for 5 min until a uniform texture was produced.
 160 The retarder admixture R42 was then slowly added while mixing continued. The rice straw
 161 fibres were gradually added to the mix together with extra water and mixing continued for 10
 162 minutes. The same procedure was applied for the control AACM mix without adding rice

163 straw fibres. Specimens for all mixes were cast in 40x40x160mm and 50x50x50mm steel
164 moulds and compacted by the vibration table in two minutes.
165 All specimens were left in the moulds covered with polythene sheets for 24 hours in the
166 laboratory air ($20 \pm 2^\circ\text{C}$, RH $65 \pm 5\%$). After 24 hours from casting, the specimens were
167 demoulded and cured in accordance with different test procedures as detailed in the next
168 section.

169 **2.4. Test procedures**

170 *2.4.1. Rice straw characteristics*

171 The properties of URS and TRS fibres were determined in accordance with procedures
172 described in [18]. SEM images of URS and TRS fibres were obtained with an ETD detector, a
173 working distance of about 10 mm, an accelerating voltage of 5 kV and a spot size of 4 nm.
174 XRD plots of URS and TRS fibres were obtained by using a Philips X-1 Pert X-ray
175 diffractometer, operated with a Cu K α radiation source (40 KV and 40 mA, wavelength
176 $\lambda=1.5406\text{nm}$ [6.07×10^{-9} 2 in.]) by scanning from 5° to 75° at an angle of 2θ , the scan step
177 size is 0.0131303. X-ray data were fitted using the pseudo-Voigt profile function and refined
178 by means of Rietveld.

179 *2.4.2. Consistency of fresh composites*

180 The workability of fresh mortar was measured with the flow table test in accordance with BS
181 EN 1015-3:1999 [23]. The flow value represented the mean diameter of a test sample of the
182 fresh mortar placed on the flow table disc by means of a defined mould and given a number of
183 vertical impacts by raising the flow table and allowing it to fall freely through a given height.

184 *2.4.3. Dry bulk density*

185 Dry bulk densities of hardened mortar were determined in accordance with BS EN 1015-
186 10:1999 [24]. Three cubes of 50x50x50mm were cast and cured in water. At 28 days age, the
187 cubes were oven dried at 60°C for 48 hours to reach the constant mass for calculation of the
188 dry bulk density.

189 *2.4.4. Mechanical properties*

190 The flexural and compressive strengths were determined in accordance with BS EN 196-1:
191 2005 [25]. After demoulding, three prisms of 40x40x160mm dimensions were used to
192 determine the flexural and compressive strength at 1 day age while another 6 prisms were
193 cured in water in the humidity room (20°C , RH45%) to determine strengths at 14 and 28 days
194 age. The three point bending test method was used to determine the flexural strengths. The
195 two halves of the broken prisms from the flexural strength tests were used to determine the
196 compressive strengths. Hence, the strength measurements of AACC were made at 1, 14 and
197 28 days age. Each result of the flexural and compressive strength was the average value of
198 three and six specimens respectively.

199 SEM (QUANTA 650) was also used to observe the bond at the straw matrix interface.
200 Samples for SEM were taken from the 28 day age specimens, oven dried for 4 hours before
201 coating with a 20 nm thick layer of gold using a Quorum Q150T. SEM images were obtained
202 with an ETD detector, a working distance of about 10 mm, an accelerating voltage of 5 kV
203 and a spot size of 4 nm.

204 XRD was used to study the effect of the treatment method of the rice straw on the
205 mineralogical compositions of alkali activated cementitious matrix at 28 days by testing
206 samples of M0, M2U, M2T. AACM matrix from broken flexural strength test samples, after
207 removing of the rice straw, was crushed by the hammer and powder was sieved under 7.5 μm
208 for XRD test samples. XRDs were conducted on a Philips X-1 Pert X-ray diffractometer.
209 They were operated with a Cu K α radiation source (40 KV and 40 mA, wavelength
210 $\lambda=1.5406\text{nm}$ [6.07×10^{-9} 2 in.]) by scanning from 5° to 75° at an angle of 2 Θ , the scan step
211 size is 0.0131303. X-ray data were fitted using the pseudo-Voigt profile function and refined
212 by means of Rietveld Refinement

213 *2.4.5. Water absorption test*

214 Test was conducted in accordance with ASTM C1403-15: Standard test method for rate of
215 water absorption of masonry mortars [26]. Three cubes of dimensions of 50x50x50mm were
216 cast and demoulded after 24 hours. After demoulding, they were put in an air tight plastic bag
217 and cured in a desiccator for 28 days before performing the water absorption test.

218 *2.4.6. Drying shrinkage*

219 The drying shrinkages of the different compositions of AACCC were determined according to
220 ASTM C596 -18: Standard test method for drying shrinkage of mortar containing hydraulic
221 cement [27]. Three prism specimens of 160mm length and 40x40 mm cross section were cast
222 and demoulded after 24 hours. Two demec points were attached on each face of the prism at a
223 gauge length of 100 mm to measure the distance (strain) between them with an extensometer.
224 The samples were then cured in water at 20°C. They were removed from water at 3 days after
225 casting, dried with a cloth and the first (datum) strain reading was taken with a demec
226 extensometer. The shrinkage specimens were then cured in the humidity room at 20°C, 45%
227 RH. Subsequent shrinkage readings were taken at regular intervals up to 90 days with the
228 extensometer.

229 *2.4.7. Durability under wet/dry cycling*

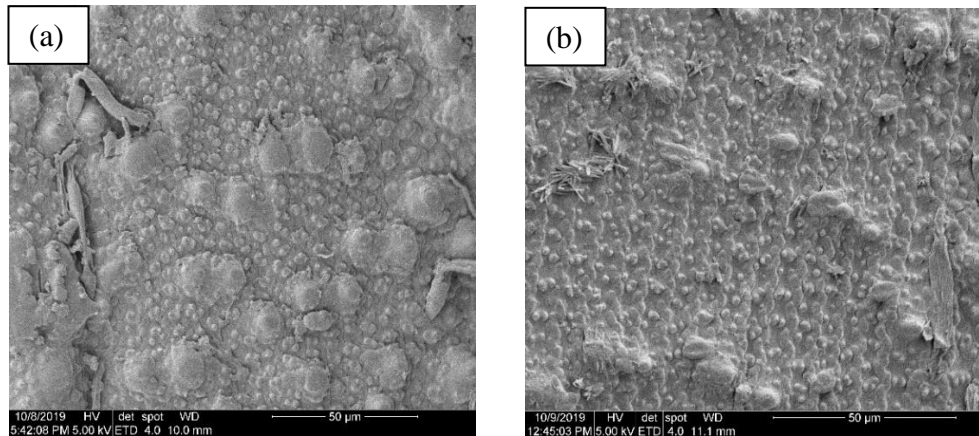
230 Wet/dry cycling tests were performed on six prisms of dimensions 40x40x160mm for each
231 mix. They were demould 24 hours after casting and cured in water until 28 days age. Three
232 prisms (set A, reference) were continuously cured in water until the test date. An other three
233 samples (set B) were subjected to wet/dry cycles. Each cycle consisted of 24 hours in water
234 at 20°C and 24 hours in the oven (60°C). The specimens were dried to attain a surface dry
235 condition before being placed in the oven, and they were also allowed to cool to room
236 temperature before being immersed in the water. Therefore, one cycle consisted of 23.5 hours
237 wet at 20°C, 0.5 hour lab air (20°C, 65%RH), 23.5 hours dry (oven, 60°C, 20%RH) and 0.5
238 hour lab air (20°C, 65%RH). At 71 days age (20 wet/dry cycles), all wet/dry curing samples
239 (set B) and water curing samples (set A) were tested to determine the flexural and
240 compressive strengths. The retained strength ratio is defined as the ratio of strength of the
241 samples after 20 wet/dry cycles curing (set B) to strength of the samples cured in water at
242 20oC, 45%RH for the duration of the durability test (set A, reference). SEM tests were also
243 conducted to determine the reason for strength loss such as bond loss at the rice straw fibre/
244 cement matrix interface or damage/strength loss of rice straw fibre or cracking of the alkali
245 activated cementitious matrix.

246 3 Results and Discussion

247 3.1. Characteristics of rice straw

248 3.1.1. SEM study

249 SEM images of URS and TRS fibres are shown in **Fig. 3**. The surface of URS fibre is quite
250 regular and covered with a layer of substance which includes oils, waxes and extractives such
251 as lipids, phenolic compounds, terpenoids, fatty acids, resin acids, etc..[18]. The surface of
252 TRS fibre is rough as the NaOH treatment removes extractives, waxes, oil and amorphous
253 constituents such as hemicellulose and lignin from fibre surfaces [28]. **It can be seen that the**
254 **surface of TRS fibres has greater roughness than the URS fibres thus promising greater bond**
255 **strength with the matrix.**
256



257
258 **Fig. 3.** SEM micrographics of (a) URS and (b) TRS

259 3.1.2 XRD study

260 XRD plots of URS and TRS fibres are presented in **Fig. 4**. There are only two clear peaks
261 appearing at around $2\theta=18^\circ$ and 22° for both URS and TRS fibres and the spectrums are very
262 similar for both type of fibres. However, it is clear that the peaks of TRS are slightly higher
263 than that of URS fibres due to the removal of the amorphous materials which agree well with
264 previous research [18]. The degree of crystalline Cellulose (I) in the total cellulose can be
265 expressed by the X-ray “crystallinity index CI” as follows [18, 29, 30] using the data in **Fig.**
266 **4**. The results are presented in **Table 3**.

$$CI = 100 \times \frac{I_{002} - I_{am}}{I_{002}}$$

267 In which: I_{002} is the intensity of the principal cellulose (I) peak at $2\theta=22^\circ$
268 I_{am} is the intensity due to the amorphous part of the sample at $2\theta=18^\circ$.
269

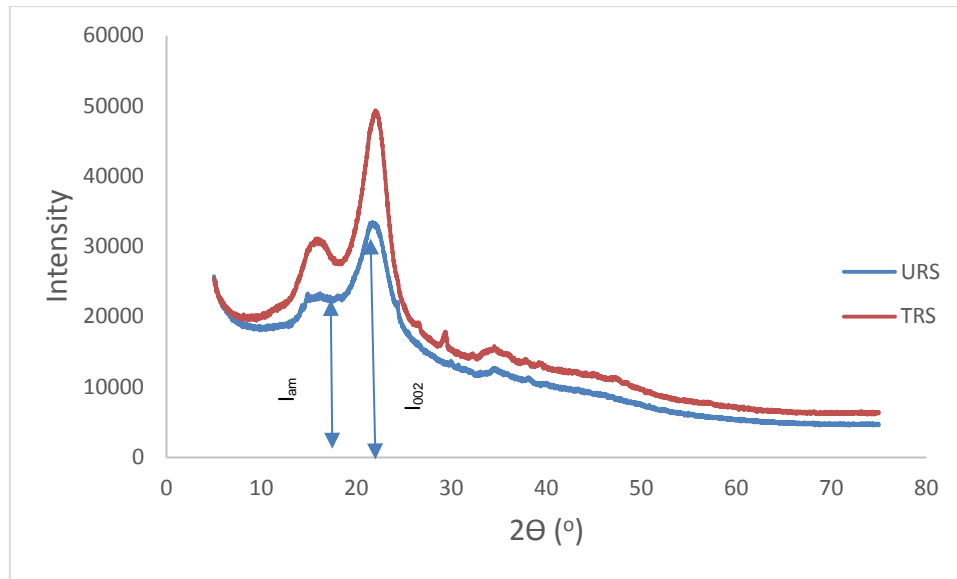


Fig. 4. X-Ray diffractograms of treated and untreated Rice straw

Table 3

Degree of crystalline cellulose of untreated and treated rice straw

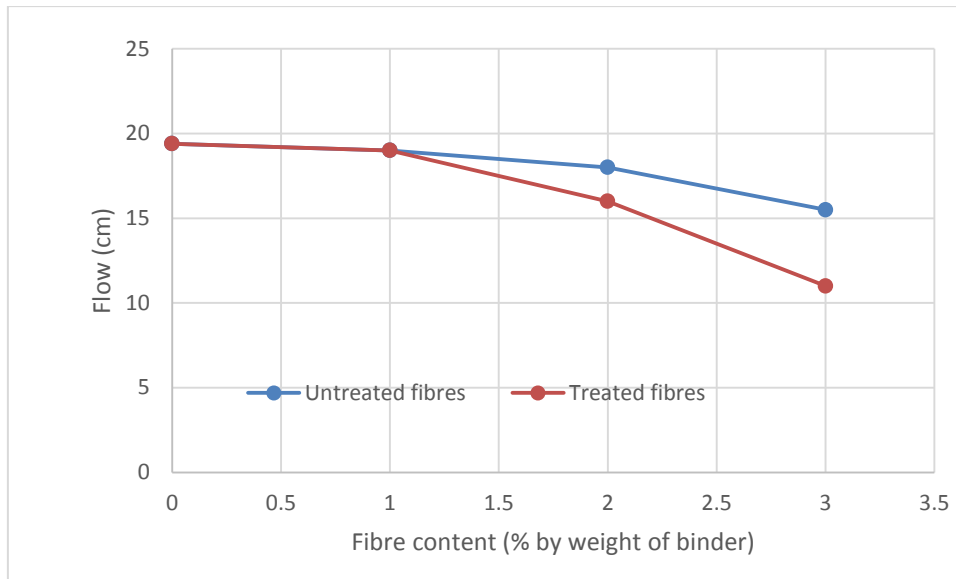
Fibres	I_{002}	I_{am}	CI (%)
Untreated rice straw (URS)	33463	22509	32.7
NaOH treated rice straw (TRS)	49372	27448	44.4

Table 3 shows that crystallinity index of TRS fibres is about 35% (from 32.7% for URS to 44.4% for TRS) higher than the URS fibres which is due to the part of the amorphous materials. This result also agrees well with the previous research conducted on rice straw sources from Egypt [18].

3.2. Workability

The flows of all mixes are given in **Fig. 5**. The rice straw fibres reduced the flow of the AACC and the workability (flows) decreased with increasing volume of rice straw fibres. The reduction in workability of rice straw composites can be due to water absorption by the hydrophilic natural fibres. The loss of workability of natural fibre composites depends mainly on the fibre aspect ratio and volume fraction in the mixtures [16]. Previous research shows that the increase in length and content of jute fibre resulted in the decrease in workability [31]. It is also reported that the workability of cement composites reduced when eucalyptus pulp, coir or eucalyptus pulp combined with sisal fibres [32] were added to the matrix.

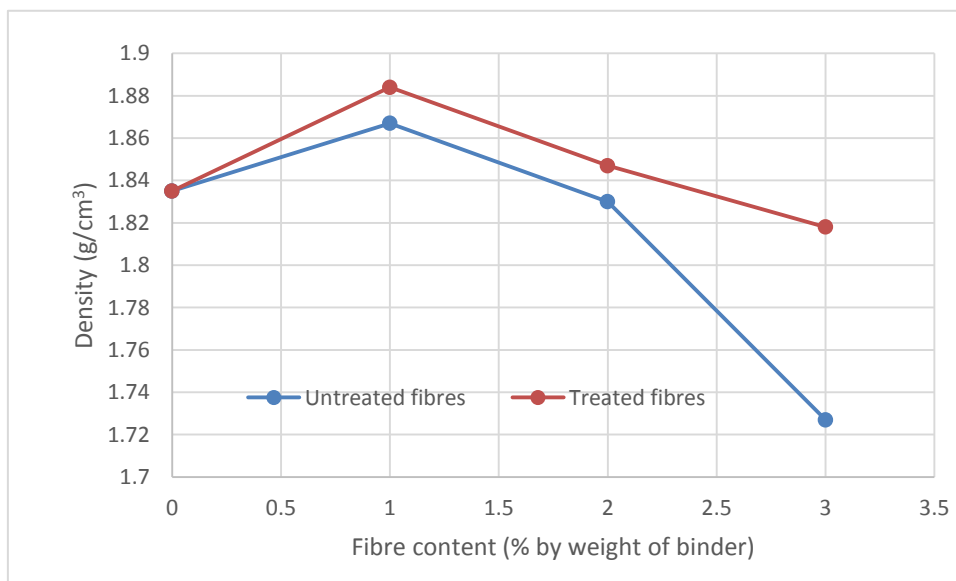
Fig. 5 also shows that the TRS fibres resulted in a higher reduction in workability than the URS fibres. This can be explained by the increase in dry surface areas of TRS fibres compared with the URS fibres (see **Fig. 2**). For improvement of workability of rice straw composites, the straw fibre can be pre-wetted before adding to the mixtures, or by consideration of the water absorption property of fibres in the mixture design [16] or using superplasticizer.



293
294 **Fig. 5.** Flow of fresh rice straw composites

295 **3.3. Dry bulk density**

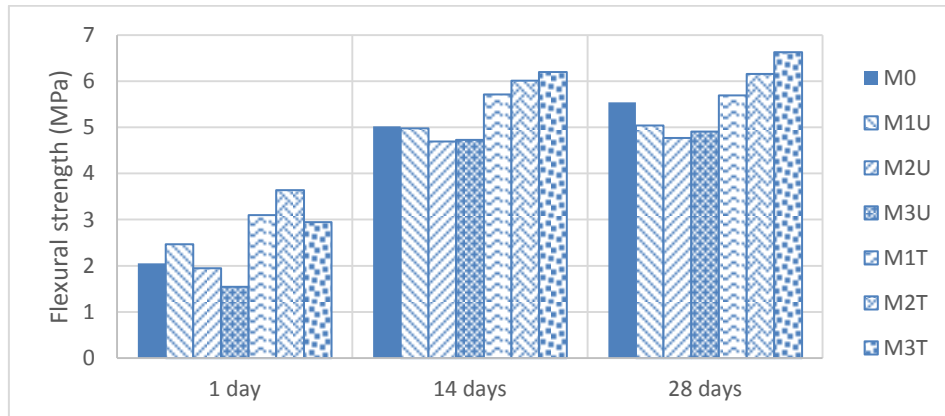
296 The dry bulk density of all composites is given in **Fig. 6**. It can be seen that 2% and 3%
 297 addition of URS reduced the density of the ACCC while there is a slight increase of density
 298 when 1% of URS is added. The alkali treated rice straw increases the density of alkali
 299 activated cementitious composites when added at the proportion of 1% and 2% by weight of
 300 binder but reduced the density of the composite when added at 3% compared with the control
 301 sample M0. This agrees well with the water absorption test results in section 3.5. Within the
 302 range of 1-3% fibre content, the density decreases with increasing rice straw fibre content for
 303 both untreated and treated fibres. The largest difference of the density between URS and TRS
 304 fibres are at 3% fibre content which is only more than 5% (from 1.727 g/cm³ for M3U to
 305 1.818 g/cm³ for M3T). It shows that the difference between density of URS and TRS
 306 composites is not significant.



307
308 **Fig. 6.** Dry bulk density of hardened rice straw composites

309 3.4 Mechanical properties

310 3.4.1 Flexural strength



311

312

Fig. 7. Flexural strengths of AACCs

313 The flexural strengths of all AACCs are plotted in **Fig. 7**. It is clear that the URS reduced the
314 flexural strength while the NaOH TRS increases the flexural strength compared with the
315 control sample without rice straw at 1 day, 14 days and 28 days, except for the increase in
316 flexural strength indicated at 1 day with the 1% of URS fibre reinforced composite. The
317 largest reductions up to 6.5% in flexural strength are at 2% of URS reinforcement (from
318 5.02MPa for M0 to 4.69MPa for M2U) at 14 days and 13.8% (from 5.54MPa for M0 to
319 4.77MPa for M2U) at 28 days. In contrast, the TRS increases the flexural strength of alkali
320 activated cementitious composites. It also been seen that at early age (1 day) the largest
321 increase in flexural strength is at 2% TRS fibres, however, at later age (14 and 28 days), it is
322 at 3% TRS. This can be explained by the aging effect on the bond of TRS fibre with the
323 matrix. Aging effect on bond has been investigated by many researchers where the bond
324 strength at steel fibre/ cement matrix interface rapidly increased with age [33, 34]. The
325 frictional bond strength of polyethylene (PE) fibre in plain and silica fume matrices under
326 moisture curing increased from 0.5 to 28 days age [35]. The increase in bond strength with
327 age is due to the increase in strength of matrix surrounding the fibres [33, 36-39]. This can
328 also be applied to the cellulose fibres as the increase in bond at rice straw fibre interface is
329 due to the increase in strength of the matrix surrounding the rice straw. Therefore, at 14 and
330 28 days age, increasing percentage of TRS results in the higher increase in flexural strength.
331 The increases in flexural strength of 3% TRS fibre composites compared with the control
332 sample are 23.5% (from 5.02MPa for M0 to 6.20MPa for the M3T) at 14 days and 19.7%
333 (from 5.54MPa for M0 to 6.63MPa for M3T) at 28 days. It is also noted that the rice straw
334 fibres fractured under flexural testing in both URS and TRS samples (see **Fig. 8**) proving that
335 the bond strength of the rice straw fibres with the matrix was higher than the tensile strength
336 of rice straw fibres.

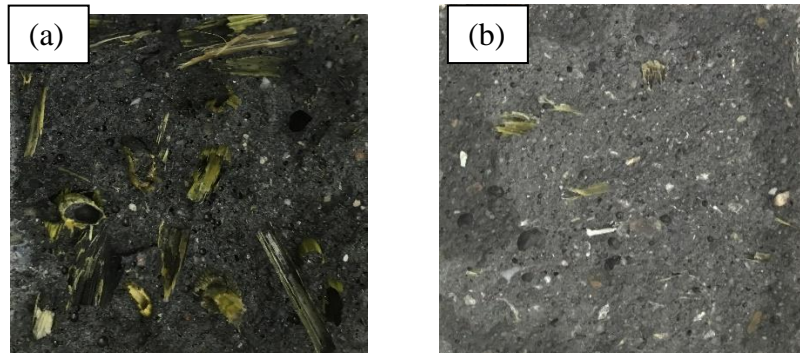


Fig. 8. Failures of a) URS and b) TRS fibres under flexural testing

3.4.2. Compressive strength

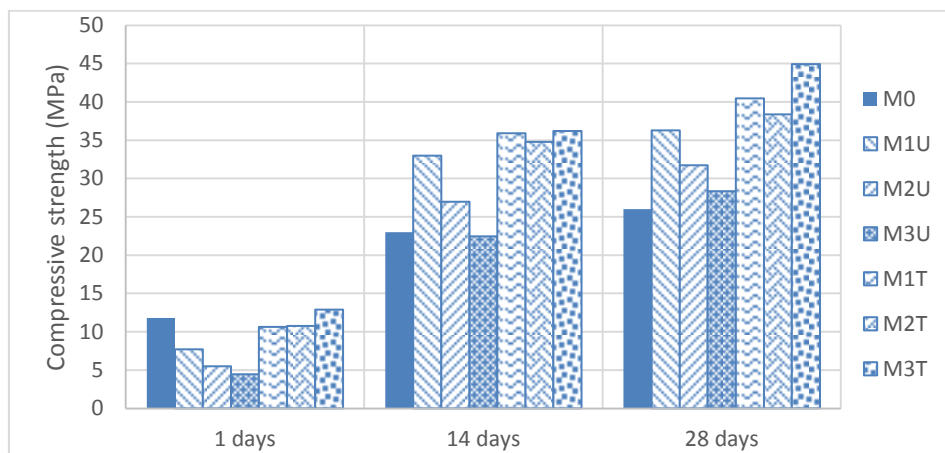


Fig. 9. Compressive strength of alkali activated cementitious composites

The compressive strengths of AACCs are shown in **Fig. 9**. The compressive strength of composites reduced at early age (1 day) when URS fibres were added to the AACM mortar, the strength decreased with increasing of fibre content. However at 14 days, 1% and 2% URS increase the compressive strength while 3% URS composite has similar strength to the control samples (M0). At 28 days, all 1%, 2% and 3% URS composites have higher compressive strengths than the control sample M0. The increase in compressive strength of URS composites compared with the control sample at 14, 28 days can again be explained by the aging effect detailed in section 3.4.1 as the increase in the strength of matrix surrounding the fibres. The optimum proportion of URS is 1% within the range of investigation with the increase in compressive strength of nearly 40% (from 26.0 MPa for the control sample M0 to 36.29MPa for the M1U) at 28 days.

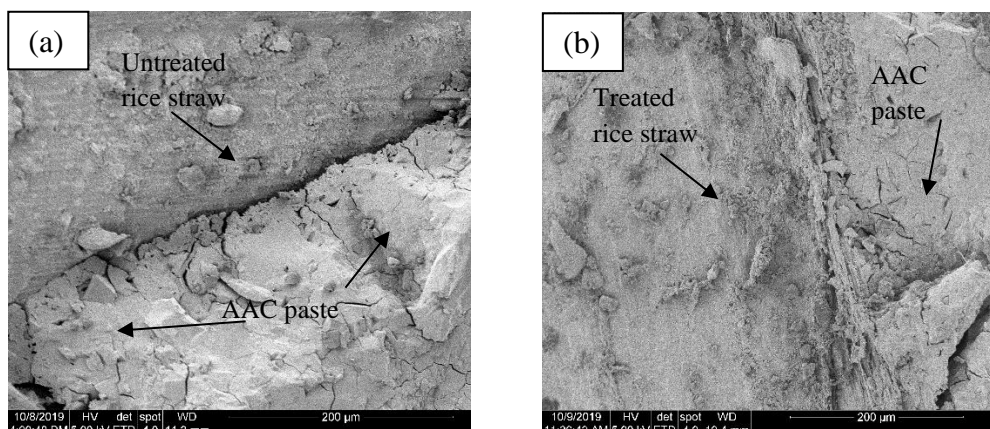
In contrast to the URS, the TRS fibres generally improve the compressive strength of the composite. At early age (1 day), 1% and 2% TRS slightly reduced the compressive strength while 3% TRS improved the compressive strength. At 14 days and 28 days, the TRS improved significantly the compressive strengths which increase with increasing straw content. The better performance of TRS fibre composite compared with the URS can be explained by the improvement of bond at the interface with the matrix due to the increase in effective surface area [22] and surface roughness as explained in detail in the next section.

360 The maximum increase in compressive strength is at 3% TRS composite which are around
361 57% (from 23.0MPa for M0 to 36.19MPa for M3T) at 7 days and 73% (from 26.0MPa for M0
362 to 44.93MPa for M3T) at 28 days. This is not in line with the density results in section 3.3 as
363 3% of both URS and TRS reduces significantly the density of the composites. The reason is
364 that the compressive strength is less affected by fibre density and also improved by the
365 hydrophilic nature of the fibres helps.

366 The compressive strength of the AAC composites is primarily controlled by the AACM
367 matrix strength. Therefore, the increase in compressive strength of AACCs compared to the
368 control can be explained by the hydrophilic nature of rice straw fibres which leads to a
369 reduction in liquid activator/ binder ratio of the matrix compared to the control. In addition,
370 the liquid activator absorbed in the rice straw fibres also works as the internal curing agent of
371 the cementitious matrix enhancing its strength. While the URS absorbed less liquid activator
372 than the TRS then this hydrophilic effect shows more effectiveness in TRS composites than
373 URS composites. This is similar to the effect of porous lightweight aggregates in concrete
374 [39].

375 3.4.3 Scanning Electron Microscope Study

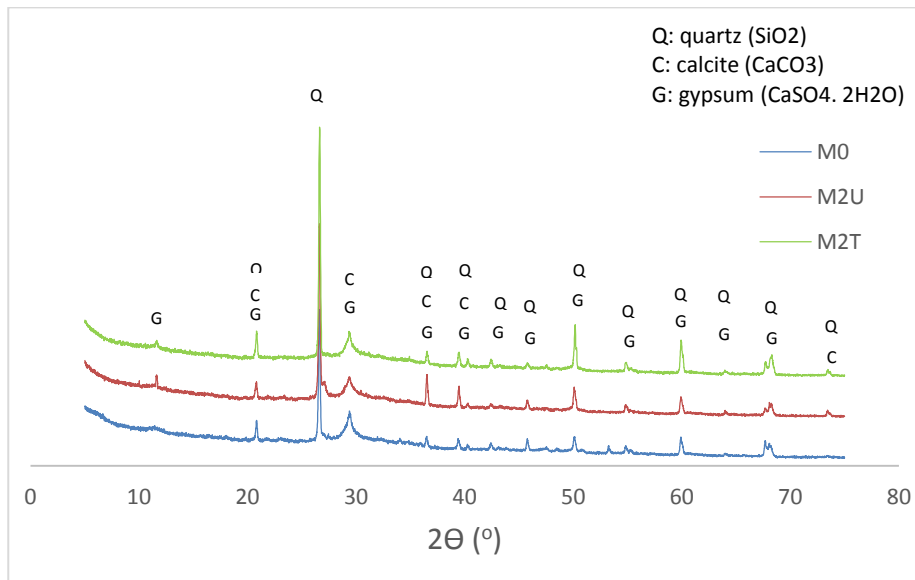
376 Bond at the fibre- matrix interface is an important factor effecting the strength of the
377 composite as the stress can be transferred from the cement matrix to the fibres throughout the
378 interface under loading [40, 41]. One of the drawbacks of using natural fibres in cementitious
379 composites is the poor bond due to the hydrophilic nature of natural fibre. The bond failure at
380 fibre and cement matrix interface under loading is due to poor chemical and physical
381 interfacial interaction between natural fibre and cement matrix [42]. The chemical treatment
382 with NaOH solution was used to eliminate lignin, natural fats, waxes and impurities from the
383 fibre surface to improve the surface roughness of natural fibres [43, 44] and surface
384 modification for enhancing the interfacial interaction [45]. The SEM images in **Fig. 10** show
385 that rice straw, after alkali treatment, improved the interfacial interaction since the gap (crack)
386 between the matrix and TRS interface (**Fig. 10b**) is quite small compared with the URS (**Fig.**
387 **10a**). In the case of TRS (**Fig.10b**) the matrix appears to have merged with the fibre at the
388 interface. It can also be seen that surface roughness of rice straw is improved significantly
389 after alkali treatment enhancing the bond strength (**Fig. 3**).



390
391 **Fig.10.** SEM images at (a) URS fibre- matrix interface and (b) TRS fibre- matrix interface

392 3.4.4. XRD Analysis

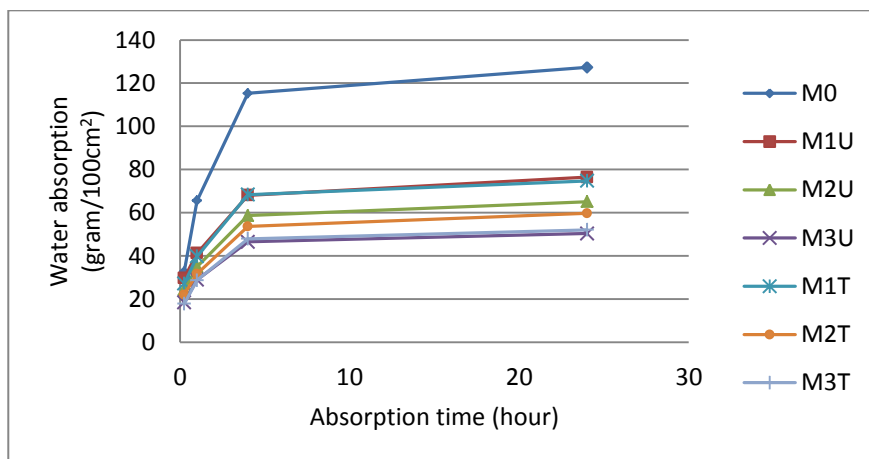
393 Mineralogical compositions of alkali activated cementitious paste at 28 days of M0, M2U,
 394 M2T are shown in **Fig. 11**. It can be seen that the XRD patterns of the three composites are
 395 very similar showing presence of quartz, calcite and gypsum. The peaks of quartz at $2\theta=27^\circ$
 396 increased slightly as rice straw was used in the composite and the peak of quartz of TRS
 397 composite is significantly higher than that of URS composite. The total CaCO_3 reduced
 398 slightly when rice straw was added to the mixes with TRS reducing CaCO_3 more than the
 399 URS. The rice straw and its treatment methods have slight influence on the mineralogical
 400 compositions of alkali activated cementitious paste. This may due to the impurity of rice
 401 straw surface and the NaOH solution used for rice straw treatment.



402

403 **Fig. 11.** X-ray diffraction patterns of AACM powder taken from the control (M0); URS
 404 composite (M2U) and TRS composite (M2T) at 28 days age

405 **3.5. Water absorption**



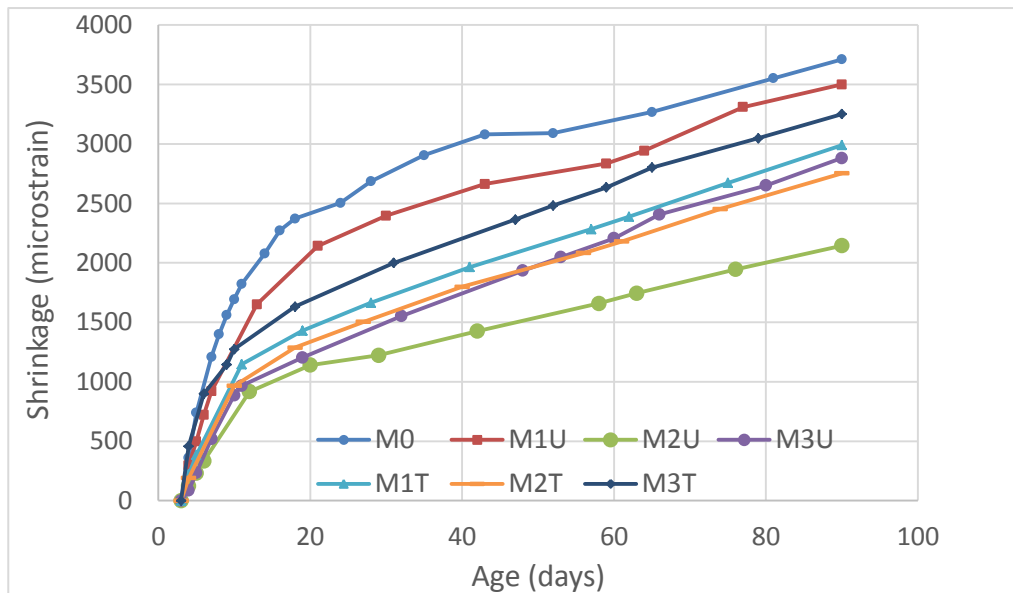
406

407 **Fig. 12.** Water absorption of alkali activated cementitious composites

408 **Fig. 12** shows that both URS and TRS reinforcement improves the water resistance of the
 409 composites. The water absorption of 1% and 3 % of both URS and TRS composites are very
 410 similar while the water absorption of 2% URS composite is slightly higher than that of TRS

411 composite. The graph also shows that increasing straw content reduces the water absorption.
 412 This agrees well with the previous research where a collated cellulose fibre at volume
 413 fractions of up to 0.5% was used in concrete and contributed to the reduction in the
 414 permeability of concrete [46]. The reduction in water absorption of fibre composites may due
 415 to the reduction in bleeding as fibres increase mix stiffness and reduce the settlement of
 416 aggregates (sand). This is also not in line with the results of the density in section 3.3 as the
 417 water absorption of the composites is less affected by fibre density, but improved by the
 418 hydrophilic nature of the fibres. Rice straw fibres absorb more liquid in the mix thereby
 419 reducing the liquid activator/binder ratio and providing the liquid as an internal curing agent.
 420 This contributes to enhanced quality of the AACM matrix (greater strength and lower
 421 porosity), thus leading to a reduction in the water absorption. The largest reduction in water
 422 absorption is up to 60% when 3% URS was added to the alkali activated cementitious mortar.

423 3.6 Drying shrinkage



424

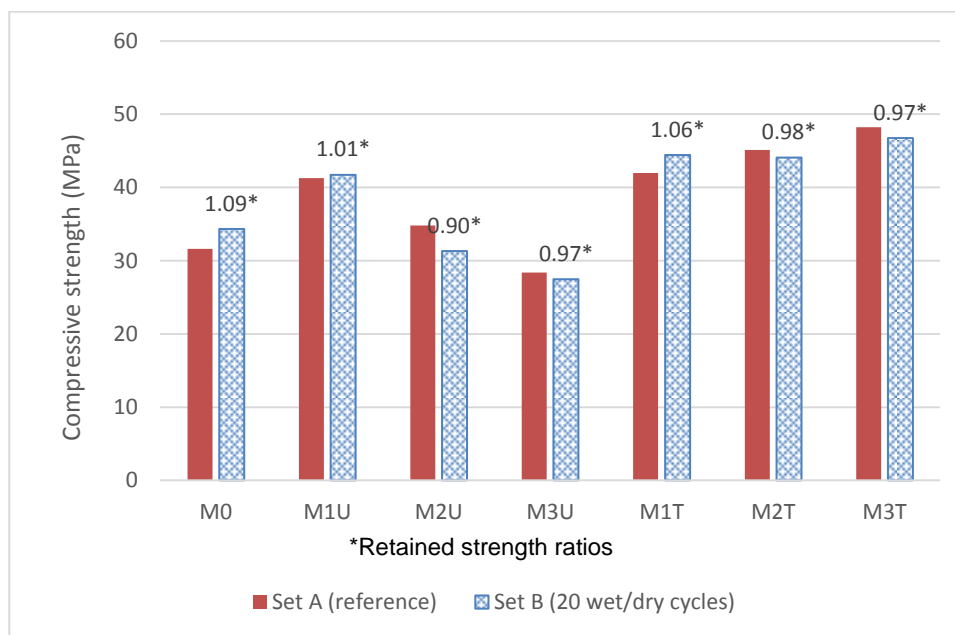
425 **Fig. 13.** Shrinkage of the alkali activated cementitious composites

426 The shrinkages of rice straw fibre AACCs (2% and 3% URS and TRS) and the control mortar
 427 up to 90 days are shown in **Fig. 13**. It is clear that both URS and TRS contributed to the
 428 reduction in drying shrinkage of the AACM mortar. It is known that the drying shrinkage is
 429 due to the evaporation of free water. **Apart from 1% rice straw fibres, the drying shrinkage of**
 430 **URS composites is less than the TRS composites and the optimum occurs at 2% URS.** At 90
 431 days the 2% URS composite (M2U) had a drying shrinkage of about 40% of the control
 432 sample (M0) This may be due to the reduction in pore volume of alkali activated cementitious
 433 composites as the rice straw was added. This is confirmed by the results of water absorption
 434 tests in section 3.4 where rice straw reduces water absorption of alkali activated cementitious
 435 composites. The reduction in drying shrinkage of rice straw composites compared to the
 436 control can also be explained by the hydrophilic effect of the straw. Rice straw absorbed the
 437 liquid and reduced the liquid activator/ binder ratio while providing internal curing enhancing
 438 the impermeability of the matrix. This leads to the reduction in drying shrinkage by reducing
 439 moisture loss from the matrix.

440 Synthetic fibres such as carbon, steel, glass have a positive effect on the drying shrinkage of
 441 cementitious mortar [47-49] while some natural plant based fibres have a negative effect on
 442 the drying shrinkage of cementitious composites [50, 51]. Previous research shows that the
 443 drying shrinkage decreases by the addition of carbon fibres depending also on the treatment of
 444 carbon fibre; it decreased by up to 32% when 0.5% of silane-treated carbon fibres, by weight
 445 of cement, were added [47]. Steel fibre also reduced shrinkage by 40% to 83% when 1-3% of
 446 fibres by volume were added [48, 49]. Previous research shows that the effect of other plant
 447 based natural fibres on the drying shrinkage of cementitious mortar depends on the fibre
 448 characteristics and fibre content leading to the effect on matrix pore structures [50]. Short
 449 sisal and coconut fibres at 2-3% volume increased drying shrinkage. The higher drying
 450 shrinkage of composites containing sisal fibre is attributed to the higher water absorption and
 451 less smooth surface of sisal fibre compared with coconut fibre [50]. Other research also
 452 reported that sisal fibre increases drying shrinkage due to the increased porosity of samples
 453 containing sisal fibre [51]. Therefore, rice straw fibre has positive effect on the reduction in
 454 drying shrinkage than other natural plant based fibres. Rice straw composite reduced drying
 455 shrinkage by up to 40% at 90 days compared with the control sample without rice straw
 456 fibres. The drying shrinkage of the rice straw fibre composites also depends on the content
 457 and treatment methods of fibres.

458 3.7. Durability under wet and dry cycling

459 3.7.1. Effect of wet dry cycling on the compressive strength



460

461

Fig. 14. Compressive strength of AACC under wet/dry cycling

462

463

464

465

466

467

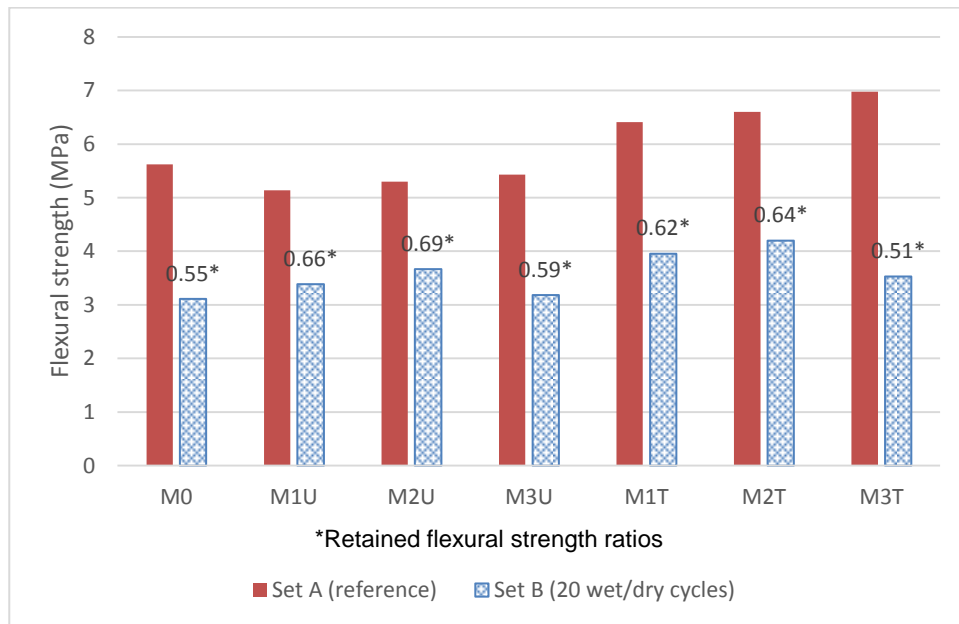
468

The compressive strengths of AACCs (M1U, M2U, M3U, M1T, M2T, M3T) and control sample (M0) of set A (reference) which were cured in water and set B (20 wet/dry cycles) are presented in Fig. 14. The retained compressive strength ratios defined as the ratio of compressive strength of the set B (20 wet/dry cycles) samples to compressive strength of the set A (reference) samples for the duration of the durability test are also presented in Fig. 14. The composites with 1% URS and 1%, 2% and 3% TRS showed an increase in the compressive strength under 20 wet/dry cycles curing compared with the control sample (M0).

469 The compressive strength of the control sample without rice straw (M0) after 20 wet/dry
 470 cycles curing is 34.31MPa while the compressive strength of 1%, 2% and 3% URS reinforced
 471 composites after 20 wet/dry cycles curing are 41.71MPa, 31.32MPa, and 27.45 MPa
 472 respectively; the compressive strength of composites reinforced with 1%, 2% and 3% TRS
 473 after 20 wet/dry cycles curing are 44.44MPa, 44.09MPa and 46.73 MPa respectively. The 3%
 474 TRS is the optimum composite for compressive strength under wet/dry cycling.

475 *3.7.2 Effect of wet dry cycling on flexural strength*

476



477

478 **Fig. 15.** Flexural strength of AACCs under wet/dry cycling

479 The flexural strengths of AACC and the control samples without rice straw fibres (M0) of
 480 set A (reference) which were cured in water and set B (20 wet/dry cycles) are presented in
 481 **Fig. 15**. The retained flexural strength ratios defined as the ratio of flexural strength of the set
 482 B (20 wet/dry cycles) samples to flexural strength of the set A samples (which were cured in
 483 water) for the duration of the durability test are also presented in **Fig. 15**. Both URS and TRS
 484 reinforcement increased the flexural strengths of composites after 20 wet/dry cycles curing
 485 compared with the control samples without fibres (M0). The flexural strength after 20
 486 wet/dry cycles curing of the control sample without fibres (M0) is 3.11MPa compared with
 487 3.39MPa, 3.67MPa and 3.18 MPa for 1%, 2%, and 3% URS fibre reinforcement respectively.
 488 The flexural strengths of 1%, 2% and 3% TRS composites after 20 wet/dry cycles curing are
 489 3.96MPa, 4.2MPa and 3.53MPa respectively.

490 The retained flexural strength ratio of control sample (M0) is 0.55 while the retained flexural
 491 strengths ratios of 1%, 2% and 3% URS composites are 0.66, 0.69 and 0.59 respectively; the
 492 retained flexural strength ratios of 1%, 2% and 3% TRS composites are 0.62, 0.64 and 0.51
 493 respectively. There were reductions in flexural strength after 20 wet/dry cycles for both the
 494 AACCs and control samples (M0).

495 The failure of all specimens under flexure occurred with the fracture of straw fibre under 20
496 wet/dry cycles (Fig. 16). Although under 20 wet/dry cycles there was visual evidence of bond
497 defect of the straw- matrix interface the residual strength was still larger than the strength of
498 the fibres.



499

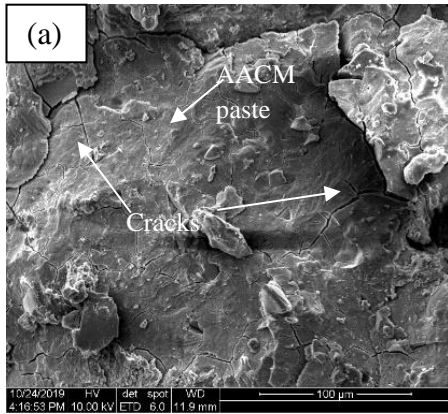
500 **Fig. 16.** Failures of treated rice straw after 20 wet/dry cycles under flexural testing

501 **Fig. 14** shows that the compressive strength of **set A (references)** which were cured in water
502 and **set B (wet/dry cycles)** of all AACCs and the control mix are similar, with the retained
503 strength ratios between 0.9 and 1.09, with most values falling between 0.97 and 1.06. This
504 indicates that the 20 wet/dry cycles exposure does not cause any significant reduction in
505 compressive strength. Since the compressive strength of the AAC composites is primarily
506 controlled by the AACM matrix strength with the rice straw fibres contributing primarily to
507 flexural strength and crack control, this indicates that the wet/dry cycles have not affected the
508 durability of the composites with respect to compressive strength. The flexural strengths of
509 the composites and the control mix M0, however, show a substantial reduction relative to **the**
510 **set A (references) which were cured in water** (see **Fig. 15**). The causes of this reduction are
511 shown in the SEM photos given in **Fig. 17**. **Fig. 17b** shows greater micro cracking in the
512 matrix of AACCs subjected to 20 wet/dry cycles compared to the continuously wet cured
513 specimens (set A) due to the high temperature curing cycle at 60deg C in the former case.
514 This micro cracking has reduced the flexural strength but the compressive strength has not
515 been similarly affected as it is less sensitive to this micro cracking. The contribution to
516 flexural strength reduction by interfacial bond loss of **URS** fibres after 20 wet/dry cycles'
517 exposure relative to **set A (reference) which were cured in water** is shown in **Figs. 17c** and
518 **17d** where a significant gap between the fibre interface and the matrix can be observed.
519 However, **Figs. 17e** and **17f** show that the bond between the TRS fibres and the AACM
520 matrix remains relatively intact under both wet/dry exposure and water curing only (set A)
521 but the fibre shows a degree of longitudinal cracking (**Fig. 17f**) due to the 60 deg C drying
522 cycle.

523 3.7.3. Mechanisms of deterioration under wet/dry cycling

524 Previous research on kraft pulp fibre–cement composites showed that under wet /dry cycling,
525 composite failure is due to the initial fibre–cement debonding due to fibre shrinkage during
526 drying, reprecipitation of relatively low-strength hydration products within the new void
527 space produced at fibre–cement interface and fibre mineralization by the re-precipitation of
528 hydration products, likely calcium hydroxide [52]. The failure mechanisms of rice straw fibre

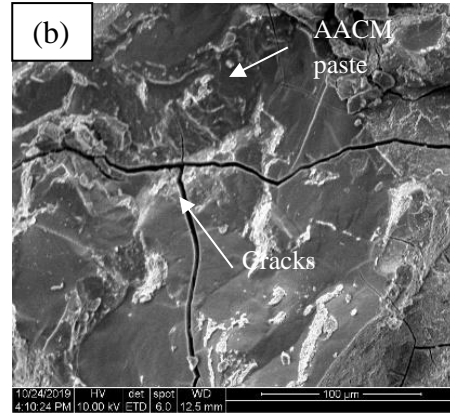
529 and cementitious matrix under wet/dry cycles can be also proposed as follows: i) initial bond
 530 failure under dry cycles as fibre shrinks during drying at high temperature; ii) new AACM
 531 products filling the void space caused by rice straw shrinkage and protecting the rice straw
 532 fibre during wet cycles iii) rice straw mineralization by the AACM products, leading to
 533 embrittlement of rice straw fibres, iv) Micro-cracks appearing in the AACM matrix under the
 534 60°C drying cycle and reducing flexural strength.



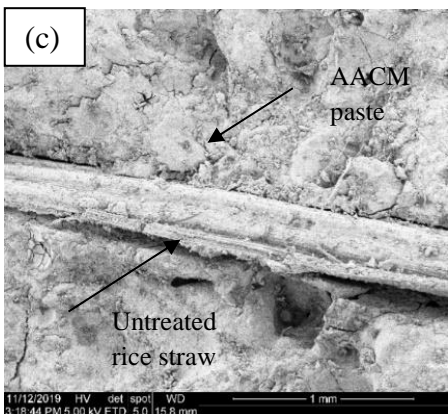
535

536

AACM (Set A)



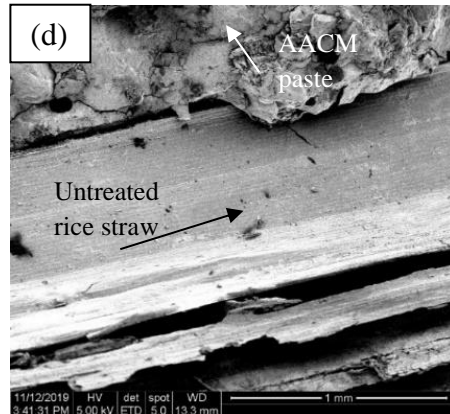
AACM (Set B, 20 wet/dry cycles)



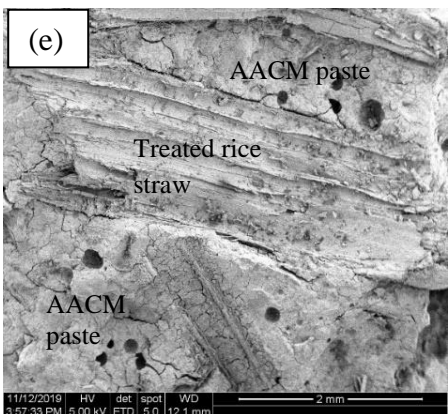
537

538

URS composite (Set A)



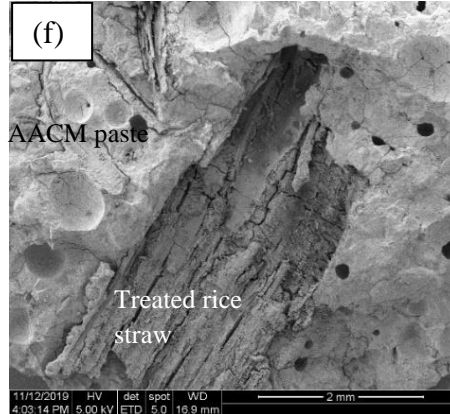
URS composite (Set B, 20 wet/dry cycles)



539

540

TRS composite (Set A)



TRS composite (Set B, 20 wet/dry cycles)

541

Fig. 17. SEMs of specimens of set A (reference) and set B (20 wet/dry cycles)

542 4. Conclusions

543 The main conclusions from the results reported in this paper are as follows:

- 544 • Alkali treatment with NaOH is an efficient method for enhancing the roughness of rice
545 straw surface leading to an improvement of bond between the rice straw fibres and the
546 alkali activated cementitious matrix.
- 547 • Both the untreated (URS) and treated (TRS) rice straw fibres with alkali reduce the
548 workability of alkali activated cementitious composites (AACC). The reduction in
549 workability of rice straw composites can be due to water absorption by the hydrophilic
550 rice straw fibres. The TRS fibres resulted in a higher reduction in workability than the
551 URS fibres since the TRS has higher dry surface areas than the URS fibres.
- 552 • The URS fibres reduce the flexural strength while TRS fibres increase the flexural
553 strength in comparison with the control sample. The better performance of TRS fibre
554 composite compared with the URS can be explained by the improvement of bond at
555 the interface with the matrix due to the increase in effective surface area and surface
556 roughness.
- 557 • Both the URS and TRS reinforcement improve the compressive strengths at 28 days
558 compared with the control. This is due to the hydrophilic nature of rice straw leading
559 to reduction in the liquid activator/binder ratio. In addition, the liquid absorbed in the
560 rice straw fibres provides an internal curing agent enhancing the strength of AACM
561 matrix. The maximum increase of 73% in compressive strength compared with the
562 control occurs at 3% TRS at 28 days.
- 563 • Both URS and TRS reduce the water absorption of alkali activated cementitious
564 composites. This may due to the reduction in bleeding as fibres increase mix stiffness
565 and reduce the settlement of aggregates (sand). Greater volume of rice straw fibres
566 leads to less water absorption. The largest reduction in water absorption is up to 60%
567 compared with the control at 3% volume of the URS fibres.
- 568 • Both URS and TRS fibres reduce the drying shrinkage of AACC. The rice straw
569 reduces the porosity of alkali activated cementitious composites because of the
570 reduction in liquid activator/binder ratio caused by the hydrophilic nature of rice straw
571 and the internal curing provided by the moisture held in the straw. The reduction in
572 porosity and the moisture trapped in the fibres reduces shrinkage. At 90 days the 2%
573 URS composite reduced the drying shrinkage by more than 40% compared with the
574 control.
- 575 • In general, 1% and 2% of both URS and TRS fibres improve the durability of AACCs
576 under wet/dry cycling as it increases the retained flexural strength ratios of the AACCs
577 (between 0.62 and 0.69) compared to the control (0.55). In addition, 1% and 2% of
578 both URS and TRS fibre reduces insignificantly the retained compressive strength
579 ratios of the AACCs (between 0.9 and 1.06) compared to the control (1.09). The
580 highest retained flexural strength ratio is found at 2% URS composites.
- 581 • Further research on the effect of different sources, lengths, treatment methods of rice
582 straw on the mechanical properties including interfacial bond to the matrix is needed
583 as these parameters are expected to contribute significantly to the properties of AACC.
- 584 • Further research is needed to analyse the functional groups of straw cellulose and the
585 binding phases within the hardened matrix of the straw composites.

586 **Acknowledgments:** The authors would like to express their gratitude for National Foundation
587 for Science and Technology Development of Vietnam (No.07/QD-HDQL-NAFOSTED)
588 within The National Foundation for Science and Technology Development (NAFOSTED) –
589 The UK Academies collaboration programme. The authors also gratefully acknowledge the
590 support of the Materials and Engineering Research Institute, Sheffield Hallam University, UK
591 and The University of Danang- University of Science and Technology, Vietnam.

592 **Funding:** This work was supported by the National Foundation for Science and Technology
593 Development of Vietnam (No.07/QD-HDQL-NAFOSTED) within The National Foundation
594 for Science and Technology Development (NAFOSTED) – The UK Academies collaboration
595 programme. Funding was also contributed by the Materials and Engineering Research
596 Institute, Sheffield Hallam University, UK to host the visiting researcher and support the
597 experimental research.

598 **Author contributions: Chinh Van Nguyen:** Methodology, Data curation, Formal analysis, ,
599 Investigation, Validation, Funding acquisition, Roles/Writing - original draft; **P.S. Mangat:**
600 Conceptualization, Resources, Supervision, Writing - review & editing.

601 **References**

- 602 [1] H. Stripple, C. Ljungkrantz, T. Gustafsson, R. Andersson, ‘CO₂ uptake in cement containing
603 products- Background and calculation models for IPCC implementation, Report number: B 2309, IVL
604 Swedish Environmental Research Institute Ltd (2018), [https://cembureau.eu/media/1753/ivl-report-](https://cembureau.eu/media/1753/ivl-report-co2-uptake-in-cement-containing-products-isbn-number-b2309.pdf)
605 [co2-uptake-in-cement-containing-products-isbn-number-b2309.pdf](https://cembureau.eu/media/1753/ivl-report-co2-uptake-in-cement-containing-products-isbn-number-b2309.pdf)
606 [2] C. Shi, P. Krivenko, D. Roy, Alkali- Activated Cements and Concretes, Taylor & Francis Group,
607 2005. [ISBN 9780415700047 - CAT# RU0043X](https://doi.org/10.1016/B978-0-08-100370-1.00018-4)
608 [3] P. Mangat, P. Lambert, Sustainability of alkali-activated cementitious materials and geopolymers,
609 in: Sustain. Constr. Mater., Elsevier Ltd (2016) 459–476, [10.1016/B978-0-08-100370-1.00018-4](https://doi.org/10.1016/B978-0-08-100370-1.00018-4).
610 [4] J.L. Provis, J.S.J. van Deventer, Alkali-Activated Materials State-of-the-Art Report, RILEM TC
611 224-AAM, 2014, [DOI: 10.1007/978-94-007-7672-2](https://doi.org/10.1007/978-94-007-7672-2)
612 [5] P. Duxson, J.L. Provis, Designing precursors for geopolymer cements, Journal of the American
613 Ceramic Society 91 (2008) 3864-3869, <https://doi.org/10.1111/j.1551-2916.2008.02787.x>
614 [6] B. Talling, P.V Krivenko, Blast furnace slag—the ultimate binder. In: Chandra, S. (Ed.), Waste
615 Materials Used in Concrete Manufacturing, Noyes Publications, Park Ridge, NJ (1996) 235–289,
616 <https://doi.org/10.1016/B978-081551393-3.50008-9>
617 [7] O.O. Ojedokun, P.S Mangat, Chloride diffusion in alkali activated concrete. In: Second
618 International Conference on Concrete Sustainability, ICCS Madrid 16 September (2016).
619 [8] C.V. Nguyen, P. S. Mangat, G. Jones, Effect of shrinkage reducing admixture on the strength and
620 shrinkage of alkali activated cementitious mortar, IOP Conf. Series: Materials Science and
621 Engineering 371 (2018) 012022 [doi:10.1088/1757-899X/371/1/012022](https://doi.org/10.1088/1757-899X/371/1/012022)
622 [9] P.S. Mangat, O.O. Ojedokun, Influence of curing on pore properties and strength of alkali
623 activated Mortars, Construction and Building Materials 188 (2018) 337–348,
624 <https://doi.org/10.1016/j.conbuildmat.2018.07.180>
625 [10] J. Davidovits, Geopolymer Chemistry and Applications. Institut Géopolymère, Saint- Quentin,
626 France (2008), [ISBN: 9782951482098 \(4th ed.\)](https://doi.org/10.1016/j.conbuildmat.2018.07.180)
627 [11] G. Rostovskaya, V. Ilyin, A. Blazhis, A, The service properties of the slag alkaline concretes. In:
628 Ertl, Z. (Ed.), Proceedings of the International Conference on Alkali Activated Materials—Research,
629 Production and Utilization, Prague, Czech Republic, Česká rozvojová agentura (2007) 593–610.
630 [12] M. Ardanuy, J. Claramunt, R. Filho, Cellulosic fibre reinforced cement-based composites: a
631 review of recent research, Constr. Build. Mater. 79 (2015) 115–128,
632 <https://doi.org/10.1016/j.conbuildmat.2015.01.035>

633 [13] F. Pacheco-Torgal, S. Jalali, Cementitious building materials reinforced with vegetable fibres: a
634 review, *Constr. Build. Mater.* 25 (2011) 575–581, <https://doi.org/10.1016/j.conbuildmat.2010.07.024>
635 [14] Z. Li, X. Wang, L. Wang, Properties of hemp fibre reinforced concrete composites, *Compos. Part*
636 *A* 37 (2006) 497–505, <https://doi.org/10.1016/j.compositesa.2005.01.032>
637 [15] S.V. Joshi, L.T. Drzal, A.K. Mohanty, S. Arora, Are natural fibres composites environmentally
638 superior to glass fibre reinforced composites?, *Compos Part A* 5 (2004) 371–376,
639 <https://doi.org/10.1016/j.compositesa.2003.09.016>
640 [16] O. Onuaguluchi, N. Banthia, Plant-based natural fibre reinforced cement composites: A review,
641 *Cement and Concrete Composites* 68 (2016) 96–108,
642 <https://doi.org/10.1016/j.cemconcomp.2016.02.014>
643 [17] F. Ataie, Influence of Rice Straw Fibers on Concrete Strength and Drying Shrinkage,
644 *Sustainability* (2018) 2445; [doi:10.3390/su10072445](https://doi.org/10.3390/su10072445)
645 [18] I.N.M Mohamed, Properties of rice straw cementitious composite, PhD Thesis, Darmstadt
646 University of Technology, Germany, 2011, <https://core.ac.uk/download/pdf/11681186.pdf>
647 [19] J. Chen, E. M.A. Elbashiry, T.Yu, Y. Ren, Z.Guo, S.Liu, Research progress of wheat straw and
648 rice straw cement-based building materials in China, *Magazine of Concrete Research* 70(2018) 84–95,
649 <https://doi.org/10.1680/jmacr.17.00064>
650 [20] S. Mishra, A.K. Mohanty, L.T. Drzal, M. Misra, G. Hinrichsen, A review on pineapple leaf
651 fibers, sisal fibers and their biocomposites, *Macromol. Mater. Eng.* 289 (2004) 955–974.
652 [doi:10.1002/mame.200400132](https://doi.org/10.1002/mame.200400132)
653 [21] D. Sedan, C. Pagnoux, A. Smith, T. Chotard, Mechanical properties of hemp fibre reinforced
654 cement: Influence of the fibre/matrix interaction, *J. Eur. Ceram. Soc.* 28 (2008) 183–192,
655 <https://doi.org/10.1016/j.jeurceramsoc.2007.05.019>
656 [22] R.D. T. Filho, F.A. Silva, E.M.R. Fairbairn, J.A. M. Filho, Durability of compression molded
657 sisal fiber reinforced mortar laminates, *Constr. Build. Mater* 23 (2009) 2409–2420,
658 <https://doi.org/10.1016/j.conbuildmat.2008.10.012>
659 [23] BS EN1015-3:1999, Methods of test for mortar for masonry- Part 3: Determination of consistence
660 of fresh mortar (by flow table), BSi British Standard (1999)
661 [24] BS EN1015-10:1999, Methods of test for mortar for masonry- Part 10: Determination of dry bulk
662 density of hardened mortar, BSi British Standard (1999)
663 [25] BS EN 196-1:2005, Method of testing cement- Part 1 Determination of strength- Compressive
664 strength, BSi British Standard (2005)
665 [26] ASTM C1403-15, Standard Test Method for Rate of Water Absorption of Masonry Mortars,
666 ASTM Int. West Conshohocken, PA, 2015
667 [27] ASTM C596-18, Standard Test Method for Drying Shrinkage of Mortar Containing Hydraulic
668 Cement, West Conshohocken, PA, 2015
669 [28] M. Troedec, D. Sedan, C. Peyratout, J. Bonneta, A. Smith, R. Guinebretiereb, V. Gloaguenc, P.
670 Krausz, Influence of various chemical treatments on the composition and structure of hemp fibres,
671 *Compos. Part A* 39 (2008) 514–522, <https://doi.org/10.1016/j.compositesa.2007.12.001>
672 [29] L. Segal, C.M. Conrad, The characterization of cellulose derivatives using x-ray diffractometry,
673 *American Dyestuff Reporter* (1957) 637–642.
674 [30] L. Segal, J.J. Creely, A.E. Martin, C.M. Conrad, An empirical method for estimating the degree
675 of crystallinity of native cellulose using the X-ray diffractometer, *Text. Resear. J* 29 (1959) 764–786.
676 [31] M.A. Mansur, M.A. Aziz, A study on jute fibre reinforced cement composites, *Int J Cem*
677 *Compos. Lightweight Concr.* 4 (2) (1982) 75–82, [https://doi.org/10.1016/0262-5075\(82\)90011-2](https://doi.org/10.1016/0262-5075(82)90011-2)
678 [32] H. Savastano, V. Agopyan, A.M. Nolasco, L. Pimentel, Plant fibre reinforced cement components
679 for roofing, *Constr. Build. Mater.* 13 (1999) 433–438, [https://doi.org/10.1016/S0950-0618\(99\)00046-X](https://doi.org/10.1016/S0950-0618(99)00046-X)
680 [33] H.V. Le, D. Moon, D.J. Kim, Effects of ageing and storage conditions on the interfacial bond
681 strength of steel fibers in mortars, *Construction and Building Materials* 170 (2018) 129–141,
682 <https://doi.org/10.1016/j.conbuildmat.2018.03.064>
683 [34] R.J. Gray, C.D. Johnston, The effect of matrix composition on fiber/matrix interfacial bond shear
684 strength in fiber-reinforced mortar, *Cem. Concr. Res.* 14 (1984) 285–296,
685 [https://doi.org/10.1016/0008-8846\(84\)90116-9](https://doi.org/10.1016/0008-8846(84)90116-9)

686 [35] Y.W. Chan, V.C Li, Age effect on the characteristics of fibre-cement interfacial properties, *J.*
687 *Mater. Sci.* 32 (1997) 5287–5292, <https://doi.org/10.1023/A:1018658626152>
688 [36] D.J. Kim, S. El-Tawil, A. Naaman, Effect of matrix strength on pullout behaviour of high-
689 strength deformed steel fibers, *ACI Spec. Publ.* (2010) 135–150.
690 [37] T. Abu-Lebdeh, S. Hamoush, W. Heard, B. Zornig, Effect of matrix strength on pullout behavior
691 of steel fiber reinforced very-high strength concrete composites, *Constr. Build. Mater.* 25 (2011) 39–
692 46, <https://doi.org/10.1016/j.conbuildmat.2010.06.059>.
693 [38] A.E. Naaman, H. Najm, Bond-slip mechanisms of steel fibers in concrete, *ACI Mater. J.* 88
694 (1991) 135–145.
695 [39] J. Browning, D. Darwin, D. Reynolds, B. Pendergrass, Lightweight aggregate as internal curing
696 agent to limit concrete shrinkage, *ACI Materials Journal.* 108 (2011) 638–644,
697 [https://www.concrete.org/publications/internationalconcreteabstractsportal/m/details/id/51683](https://www.concrete.org/publications/internationalconcreteabstractsportal/m/details/id/51683467)
698 [467](https://www.concrete.org/publications/internationalconcreteabstractsportal/m/details/id/51683467)
699 [40] L.Q.N. Tran, C.A. Fuentes, C. Dupont-Gillain, Understanding the interfacial compatibility and
700 adhesion of natural coir fibre thermoplastic composites, *Compos. Sci. Tech* 80 (2013) 23–30,
701 [doi: 10.1016/j.compscitech.2013.03.004](https://doi.org/10.1016/j.compscitech.2013.03.004)
702 [41] B.L.S. Sipião, L.S. Reis, R.D.L.M. Paiva, M.R. Capri, D.R. Mulinari, Interfacial adhesion in
703 natural fiber-reinforced polymer composites. In *Lignocellulosic Polymer Composites: Processing,*
704 *Characterization and Properties;* Wiley: New York, USA (2014) 17-
705 39, <https://doi.org/10.1002/9781118773949.ch2>
706 [42] M. Hao, H. Wu, F. Qiu, X. Wang, Interface bond improvement of sisal fibre reinforced
707 polylactide composites with added epoxy oligomer, *Materials* 11 (2018) 398,
708 [doi:10.3390/ma11030398](https://doi.org/10.3390/ma11030398)
709 [43] N. Sgriccia, M.C. Hawley, M. Misra, Characterization of natural fiber surfaces and natural fiber
710 composites, *Compos. Part A Appl. Sci. Manuf* 39 (2008) 1632–1637,
711 <https://doi.org/10.1016/j.compositesa.2008.07.007>
712 [44] G.N. Farahani, I. Ahmad, Z. Mosadeghzad, Effect of fiber content, fiber length and alkali
713 treatment on properties of kenaf fiber/UPR composites based on recycled PET wastes, *Polym. Plast.*
714 *Technol. Eng* 51(2012) 634–639, <https://doi.org/10.1080/03602559.2012.659314>
715 [45] B.L.S. Sipião, L.S. Reis, R.D.L.M. Paiva, M.R. Capri, D.R. Mulinari, Chemical modification and
716 properties of cellulose-based polymer composites. In *Lignocellulosic Polymer Composites:*
717 *Processing, Characterization and Properties;* Wiley: New York, USA (2014) 301–323,
718 <https://doi.org/10.1002/9781118773949.ch14>
719 [46] N. Banthia, A. Bhargava, Permeability of stressed concrete and role of fiber reinforcement, *ACI*
720 *Mater J.* 104 (1) (2007) 70–76.
721 [47] Y. Xu, D.D.L. Chung, Reducing the drying shrinkage of cement paste by admixture surface
722 treatments, *Cement and Concrete Research* 30 (2000) 241–245, [https://doi.org/10.1016/S0008](https://doi.org/10.1016/S00088846(99)00239-2)
723 [8846\(99\)00239-2](https://doi.org/10.1016/S00088846(99)00239-2)
724 [48] P. S. Mangat, M.M. Azari, Shrinkage of steel fibre reinforced cement composites, *Materials and*
725 *Structures* 21 (1988),163-171, <https://doi.org/10.1007/BF02473051>
726 [49] E.T. Dawood, M. Ramli, High strength characteristics of cement mortar reinforced with hybrid
727 fibres, *Construction and Building Materials* 25 (2011) 2240–2247,
728 <https://doi.org/10.1016/j.conbuildmat.2010.11.008>
729 [50] R.D. Toledo Filho, K. Ghavami, M.A. Sanjuan, G.L. England, Free, restrained and drying
730 shrinkage of cement mortar composites reinforced with vegetable fibres, *Cem. Concr. Compos.* 27
731 (2005) 537e546, <https://doi.org/10.1016/j.cemconcomp.2004.09.005>
732 [51]] F.A. Silva, R.D. Toledo Filho, J.A. Melo Filho, E.M.R. Fairbairn, Physical and mechanical
733 properties of durable sisal fibre-cement composites, *Constr. Build. Mater* 24 (2010) 777–785,
734 <https://doi.org/10.1016/j.conbuildmat.2009.10.030>.
735 [52] B.J. Mohr, H. Nanko, K.E. Kurtis, Durability of kraft pulp fiber–cement composites to wet/dry
736 cycling, *Cement & Concrete Composites* 27 (2005) 435–448,
737 <https://doi.org/10.1016/j.cemconcomp.2004.07.006>